Catalytic Partial Oxidation of Methane over Ni-Based Catalysts Derived from Ni-Mg/Al Ternary Hydrotalcites

ARTICLE *in* ENERGY & FUELS · FEBRUARY 2009

Impact Factor: 2.79 · DOI: 10.1021/ef800933j

Catalytic Partial Oxidation of Methane over Ni-Based Catalysts Derived from Ni−Mg/Al Ternary Hydrotalcites

Zheng Jiang,[†] Jixin Su,[‡] Martin Owen Jones,[†] Huahong Shi,[†] Tiancun Xiao,*[,†] and Peter P. Edwards*[,†]

Inorganic Chemistry Laboratory, University of Oxford, South Parks Road, OX1 3QR, Oxford, U.K., and School of Environmental Science and Engineering, Shandong University, Jinan, 250100, Shandong, P.R. China

Received October 25, 2008. Revised Manuscript Received January 2, 2009

Ni-based catalysts derived from Ni−Mg/Al ternary hydrotalcites with low Ni-loadings have been prepared for the partial oxidation of methane (POM) to syngas. The reducibility, surface basicity, and effects of catalyst reduction on POM reactivity over these catalysts have been explored. Temperature-programmed reduction and CO_2-temperature-programmed desorption results indicate that the amount of Ni-loading and the Mg/Al molar ratio exert a remarkable influence on their reducibility but have little influence on the surface basicity, with an increase in Mg/Al ratio also lessening the base strength of the alkaline sites. Reaction temperature significantly affects the reactivity of the catalysts, and high temperature reduction of the catalysts can lead to superior reactivity to those reduced at low temperature. An in situ reduction of the catalyst has been observed in the POM reaction for catalysts reduced at low temperature. Under the optimized reaction conditions, the catalysts with Ni content from 8 wt % to 15.5 wt % show similar activity in POM reactions, and this activity is much higher than for catalysts with lower Ni-loading (∼4 wt %), which is explained in terms of nickel reducibility and the surface basicity of the catalysts.

1. Introduction

The catalytic partial oxidation of methane (POM) has been extensively investigated because of its unique features:[1,2] (a) a mild exothermic reaction,[3] which is energy efficient; (b) very short residence time (around a few milliseconds) on the surface of catalysts;[4] (c) high methane conversions and selectivity of CO and H_2; and (d) the H_2/CO molar ratio in the produced syngas of about 2, which is particularly favorable for methanol synthesis and Fischer−Tropsch synthesis.[5,6] Moreover, the recent developments of solid state oxide fuel cells fueled with syngas also greatly stimulated the researches of POM.[7] According to the results of previous investigations and the proposed reaction mechanisms,[6] the ideal catalysts should mainly be of such features: (1) high dispersed active sites favoring the POM activity and selectivity; (2) suitable surface basicity which greatly influences the adsorption−desorption of the intermediates and thus performance of the catalysts; and (3) sustainability of POM catalysts which depends on the thermally stability of the catalysts or supports. So far, numerous transition-metal[6−9] and noble-metal[4,10−12] catalysts have been explored for the POM reaction. Although the latter have been reported to be more active and less sensitive to carbon deposition than the former, they are not practical from the industrial viewpoint because of their high cost and limited availability of resources. Among transition metal catalysts, Ni-based catalysts attract extensive attention because of their excellent reactivity, wide availability, and low cost.[6,13] However, the traditional Ni/Al_2O_3 suffers from poor stability and rapid deactivation because of carbon deposition, sintering, and the formation of $NiAl_2O_4$.[6,14] Moreover, in some special engineering processes, for example, partial oxidation of methane in fluidized bed reactors, the conventional Ni/Al_2O_3 catalysts may not be reliable because of the loss of outer layer Ni and its low fluidity.[15−18]

To tackle the problems offered by the use of low-cost Ni-based catalysts, researchers have developed various strategies, such as changing supports, the use of different precursors and pretreatments, optimizing preparation procedures, adding metal

* To whom correspondence should be addressed. E-mail: xiao.tiancun@chem.ox.ac.uk or peter.edwards@chem.ox.ac.uk.

[†] University of Oxford.

[‡] Shandong University.

(1) Hu, Y. H.; Ruckenstein, E.; Gates, B. C.; Helmut, K. *Adv. Catal.* **2004**, *48*, 297–345.

(2) York, A. P. E.; Xiao, T.-C.; Green, M. L. H.; Claridge, J. B. *Catal. Rev.* **2007**, *49*, 511–560.

(3) Basile, F.; Basini, L.; Amore, M. D.; Fornasari, G.; Guarinoni, A.; Matteuzzi, D.; Piero, G. D.; Trifir, F.; Vaccari, A. *J. Catal.* **1998**, *173*, 247–256.

(4) Hickman, D. A.; Schmidt, L. D. *J. Catal.* **1992**, *138*, 267–282.

(5) Shishido, T.; Sukenobu, M.; Morioka, H.; Kondo, M.; Wang, Y.; Takaki, K.; Takehira, K. *Appl. Catal., A* **2002**, *223*, 35–42.

(6) Christian Enger, B.; Lødeng, R.; Holmen, A. *Appl. Catal., A* **2008**, *346*, 1–27.

(7) Chaniotis, A. K.; Poulikakos, D. *J. Power Sources* **2005**, *142*, 184–193.

(8) Hao, Z.-p.; Hu, C.; Jiang, Z.; Lu, G. Q. *J. Environ. Sci.* **2004**, 7.

(9) Lucredio, A. F.; Jerkiewickz, G.; Assaf, E. M. *Appl. Catal., A* **2007**, *333*, 90–95.

(10) Li, D.; Shiraga, M.; Atake, I.; Shishido, T.; Oumi, Y.; Sano, T.; Takehira, K. *Appl. Catal., A* **2007**, *321*, 155–164.

(11) Yang, M.; Papp, H. *Catal. Today* **2006**, *115*, 199–204.

(12) Basile, F.; Fornasari, G.; Gazzano, M.; Kiennemann, A.; Vaccari, A. *J. Catal.* **2003**, *217*, 245–252.

(13) Hao, Z.; Zhu, Q.; Lei, Z.; Li, H. *Powder Technol.* **2008**, *182*, 474–479.

(14) Dissanayake, D.; Rosynek, M. P.; Kharas, K. C. C.; Lunsford, J. H. *J. Catal.* **1991**, *132*, 117–127.

(15) Ji, Y.; Li, W.; Xu, H.; Chen, Y. *Appl. Catal., A* **2001**, *213*, 25–31.

(16) Ostrowski, T.; Giroir-Fendler, A.; Mirodatos, C.; Mleczko, L. *Catal. Today* **1998**, *40*, 191–200.

(17) Wurzel, T.; Mleczko, L. *Chem. Eng. J.* **1998**, *69*, 127–133.

(18) Santos, A.; Menéndez, M.; Santaríana, J. *Catal. Today* **1994**, *21*, 481–488.

10.1021/ef800933j CCC: $40.75
Published on Web 02/18/2009

Table 1. Composition of the Ni/Mg/Al Hydrotalcite Precursors

sample	designed Ni/Mg/Al mol ratio	designed M^{2+}/M^{3+}	formula of Ni−Mg/Al ternary hydrotalcites deduced from ICP-AES and TGA results
NMA1-HT	1/11/4.0	3	$[Ni_{0.058}Mg_{0.733}Al_{0.209}(OH)_2](NO_3)_{0.209}\cdot 0.645H_2O$
NMA2-HT	1/11/3.0	4	$[Ni_{0.060}Mg_{0.774}Al_{0.166}(OH)_2](NO_3)_{0.166}\cdot 0.531H_2O$
NMA3-HT	1/11/2.4	5	$[Ni_{0.061}Mg_{0.804}Al_{0.135}(OH)_2](NO_3)_{0.135}\cdot 0.515H_2O$
NMA4-HT	0.4/11/2.4	4.75	$[Ni_{0.026}Mg_{0.829}Al_{0.145}(OH)_2](NO_3)_{0.145}\cdot 0.498H_2O$
NMA5-HT	1.9/11/2.4	5.375	$[Ni_{0.115}Mg_{0.752}Al_{0.133}(OH)_2](NO_3)_{0.133}\cdot 0.539H_2O$

or oxide promoters, and so forth.[6] Because carbon formation is structure sensitive on Ni catalysts,[19,20] modifications are typically performed to reduce the crystallite sizes and stabilize these against sintering. Noble metals have proved effective promoters for restraining carbon deposition but prone to sintering, and they are also expensive.[21] Rare earth oxides and alkaline metal oxides, mainly La and Mg, are important promoters in simultaneously inhibiting carbon deposition and improving stability of Ni-based catalysts.[8,9,22] Unfortunately, the La promoter can only be effective in a small range, with higher La loading (>2 wt %) increasing carbon deposition.[22] In contrast, the MgO promoter not only inhibits the carbon deposition but also increases the stability of the Ni/Al_2O_3 catalysts even at higher MgO content.[9] The performances of MgO modified Ni-based catalysts depend on the synthesis methods and amounts of Ni and MgO loading.[3,23,24] It has been shown that the Ni-containing hydrotalcites (HTLCs) would be promising precursors for preparation of Ni-based catalysts with desired properties, such as the high dispersion of elements, large surface area, finite particle size, high stability, and facile synthesis.[3,5,10,23] Furthermore, the controllable catalyst size and homogenously distributed and stable Ni active sites on the catalysts derived from Ni-containing hydrotalcite would be attractive for fluidized bed applications, where the pressure drop due to accumulation of particulates or carbon may be less problematic.

Hydrotalcites have been found, after thermal treatment, to afford a homogeneous dispersion of the metal and a better resistance to sintering than the corresponding alternately supported catalysts.[25] They are represented by the general formula $[M_{1-x}^{2+}M_x^{3+}(OH)_2]^{x+}[A_{x/n}]^{n-}\cdot mH_2O$, where the M^{2+} and M^{3+} are metal cations, A is an anion, n is the charge of the anion, and m is the number of interlayer water molecules.[26−29] Shishido and his co-workers [5,24] reported that the mixed oxides derived from the Ni-based hydrotalcites can minimize the carbon formation during POM reaction; however, serious carbon deposition and consequentially rapid deactivation has been observed despite the higher conversion and selectivity shown by catalysts with higher Ni loading (e.g., 20 wt %).[3] It is also reported that the Ni/Al_2O_3 catalyst with 10 wt % Ni loading displayed higher specific activity and stability in methane-CO_2 reforming than that with 20 wt % Ni loading in fluidized bed or fixed bed reactors,[13] whereas little is reported on catalysts with low Ni content and the effects of Mg/Al ratio in the hydrotalcite-derived catalysts. Tichit et al.[30] investigated the stability and the reducibility correlation between Ni and Mg/Al concentrations. They found that the reducibility of Ni decreases both with increasing Al and with increasing Mg content of the Ni/MgAl(O) catalysts, but they did not study POM reactivity nor the relationship between performance and components. Casenave et al.[25] studied the acid−base character of Ni/Mg/Al-mixed oxides with various Ni-loadings at fixed (Mg + Ni)/Al = 2 using adsorption calorimetry, but did not provide any catalytic performance data for the catalysts. Most recently, Råberg et al.[31] found a volcano-type correlation between support basicity and intrinsic catalyst activity for propane reforming to syngas over Ni/MgAl(O) catalysts derived from hydrotalcites. So far, no report has been available for POM reaction over the reduced mixed oxides derived from Ni−Mg/Al ternary hydrotalcites with lower Ni contents or for the correlation between POM reactivity and surface basicity or reducibility of the catalysts.

Here, we report the preparation of Ni-based catalysts via the reduction of mixed oxides derived from Ni−Mg/Al ternary hydrotalcites with a variety of Ni contents (4 wt %−15 wt %) and the influences of Mg/Al ratio, reduction conditions, and surface basicity on their POM performance.

2. Experimental Section

2.1. Synthesis of Ni-Based Catalysts Derived from Ni−Mg−Al Ternary Hydrotalcites. *2.1.1. Synthesis of Ni−Mg−Al Ternary Hydrotalcites.* A simple co-precipitation process is adopted to prepare Ni−Mg−Al ternary hydrotalcites (HTLCs).[26] The composition of the series of HTLCs is listed in Table 1. Typically, $Mg(NO_3)_2\cdot 6H_2O$, $Ni(NO_3)_2\cdot 6H_2O$, and $Al(NO_3)_2\cdot 9H_2O$ were dissolved in the desired amounts into 250 mL of distilled water to form solution A, and solution B is a 2 $mol\cdot L^{-1}$ NaOH solution. The solution A and B were simultaneously added to 300 mL of distilled water in a four-necked flask under vigorous stirring, under a N_2 atmosphere introduced as protective gas to minimize the presence of CO_2. All of the deionized water was microwave heated and then cooled to room temperature in a closed vessel prior to use to degas any dissolved CO_2. Careful control of the mixing rate of solution A and B maintained the pH in the 9−10 range. After continuously stirring and aging overnight, the resultant slurry was filtered and washed to pH 7. The resultant gel dried at 60 °C for 48 h to give Ni−Mg/Al HTLCs. The obtained HTLCs are denoted as NMA*i*-HT, where *i* is the label of sample, HT is hydrotalcite.

2.1.2. Synthesis of Ni-MgO/Al_2O_3 Catalysts. For the preparation of the reduced Ni-based catalysts, the as-prepared NMA-hydrotalcites were further calcined at 500 °C. The resultant Ni-based catalysts were denoted as NMA*i*-*t*, where *i* is the label of samples and *t* is the calcination temperature.

(19) Bengaard, H. S.; Nørskov, J. K.; Sehested, J.; Clausen, B. S.; Nielsen, L. P.; Molenbroek, A. M.; Rostrup-Nielsen, J. R. *J. Catal.* **2002**, *209*, 365–384.
(20) Christensen, K. O.; Chen, D.; Lødeng, R.; Holmen, A. *Appl. Catal., A* **2006**, *314*, 9–22.
(21) Li, D.; Shishido, T.; Oumi, Y.; Sano, T.; Takehira, K. *Appl. Catal., A* **2007**, *332*, 98–109.
(22) Cao, L.; Chen, Y.; Li, W. *Stud. Surf. Sci. Catal.* **1997**, *107*, 467–471.
(23) Arpentinier, P.; Basile, F.; del Gallo, P.; Fornasari, G.; Gary, D.; Rosetti, V.; Vaccari, A. *Catal. Today* **2006**, *117*, 462–467.
(24) Shishido, T.; Sukenobu, M.; Morioka, H.; Furukawa, R.; Shirahase, H.; Takehira, K. *Catal. Lett.* **2001**, *73*, 21–26.
(25) Casenave, S.; Martinez, H.; Guimon, C.; Auroux, A.; Hulea, V.; Cordoneanu, A.; Dumitriu, E. *Thermochim. Acta* **2001**, *379*, 85–93.
(26) Jiang, Z.; Hao, Z.; Yu, J.; Hou, H.; Hu, C.; Su, J. *Catal. Lett.* **2005**, *99*, 157–163.
(27) Goh, K.-H.; Lim, T.-T.; Dong, Z. *Water Res.* **2008**, *42*, 1343–1368.
(28) Kung, H. H.; Ko, E. I. *Chem. Eng. J. Biochem. Eng. J.* **1996**, *64*, 203–214.
(29) Cavani, F.; Trifir, F.; Vaccari, A. *Catal. Today* **1991**, *11*, 173–301.
(30) Tichit, D.; Medina, F.; Coq, B.; Dutartre, R. *Appl. Catal., A* **1997**, *159*, 241–258.
(31) Råberg, L. B.; Jensen, M. B.; Olsbye, U.; Daniel, C.; Haag, S.; Mirodatos, C.; Sjåstad, A. O. *J. Catal.* **2007**, *249*, 250–260.

2.2. Characterizations. *2.2.1. Powder X-ray Diffraction (XRD).* The XRD data were collected on a Rigaku D/max-2500 diffractometer with Cu Kα radiation (40 kV and 100 mA) in the scan range of $5° \leq 2\theta \leq 70°$.

2.2.2. Inductively Coupled Plasma Atomic Emission Spectrometry (ICP-AES) and Thermal Gravimetric-Differential Thermal Analysis (TG-DTA). The compositions of the catalysts were analyzed by ICP-AES (IRIS Advantage,TJA Solution). To accomplish this measurement, the sample was quantified with great accuracy using standard stock solutions. The solution was initially vaporized to remove any silicon fluoride arising from dissolving solid samples. The remaining residue was then dissolved in 0.2 mol L^{-1} hydrogen chloride, and the formed solution adjusted to weak acidity using gaseous ammonia. The resulting solution was finally diluted with deionized water.

TG-DTA (TG-2,DTA-1700, PE) was used to determine the amount of water present in the HTLC structure and to analyze the evolution of the ternary HTLCs during annealing.

2.2.3. Temperature-Programmed Reduction (TPR). The reducibility of the calcined hydrotalcite-derived catalyst was measured by the TPR method with a home-built apparatus fitted with a foreline cold trap consisting of liquid nitrogen and acetone to dry gases prior use. A 50 mg quantity of the catalyst (20−40 mesh) was mounted in a quartz tube and calcined in argon flow at 773 K for 1 h (temperature-programmed rate of 10 K min^{-1}) to remove any physisorbed substances. The sample was then cooled to ambient temperature in argon before being heated at a rate of 10 K min^{-1} in flowing (30 mL min^{-1}) hydrogen/argon (6% H_2 in Argon). The hydrogen consumed during the reduction was detected by a thermal conductivity detector (TCD).

2.2.4. CO_2 Temperature-Programmed Desorption (CO_2-TPD). The basicity of the calcined samples was determined by studying the temperature programmed desorption (TPD) of CO_2 using with a home-built apparatus equipped with a thermal conductivity detector (TCD). A small amount of each sample was first purged in situ at 450 °C with He, cooled to 100 °C, and then reacted with flowing CO_2 under isothermal conditions and subsequently cooled to room temperature. The TPD of CO_2 from these samples was then recorded by heating the samples under He flow from room temperature to 600 °C (ramp, 10 °C/min). The nature of evolved gases was dynamically determined by Gas Chromotography equipped with a TCD.

2.3. Catalytic Activity. Catalytic activity was measured at atmospheric pressure in a tubular quartz reactor (6 mm inner diameter) heated in a resistive electric oven with quartz wool used as support for the catalytic bed. Temperature was monitored using a K-type thermocouple and flow rate of gases adjusted using mass flow controllers (Beijing, D07−11/ZM and D07−7A/ZM for CH_4 and O_2 control, respectively). The analysis of the evolved products was carried out online in a Sepu-2060 (Beijing) chromatograph with a thermal conductivity detector, using a Carbosphere column.

The samples (60 mg, 40∼60mesh) were reduced in situ at 750 °C for 2 h, using a N_2/H_2 mixture containing 50% of hydrogen. To study the influence of reduction temperature, some samples were also reduced at 500, 700, 750, and 800 °C. After the reduction, a reaction mixture consisting of $CH_4/O_2/N_2$ with a molar ratio of 2:1:9 and with a total flow rate of 150 cm^3/min was supplied to the reactor. Under these conditions, the gas hourly spatial velocity (GHSV) corresponds to 120,000 h^{-1}. The large amount of N_2 introduced into the reactant mixture is to mimic the flue gas of coal-fired power plants, where very small quantities of oxygen are present.[32]

The CH_4 and O_2 conversion values (XCH_4, XO_2, respectively), and CO and H_2 selectivities (S_{CO} and S_{H2}) were calculated according to the following formulas:

$$X_{CH4} = \frac{F_{CH4,in} - F_{CH4,out}}{\sum CH_{4,in}} \times 100\% = \frac{F_{CO,out} + F_{CO2,out}}{F_{CO,out} + F_{CO2,out} + F_{CH4,out}} \times 100\% \quad (1)$$

$$X_{O2}(\%) = \frac{F_{O2,in} - F_{O2,out}}{F_{O2,in}} \times 100\% = \frac{0.5F_{CO,out} + 0.5F_{H2O,out} + F_{CO2,out}}{0.5F_{CO,out} + 0.5F_{H2O,out} + F_{CO2,out} + F_{O2,out}} \times 100\% \quad (2)$$

$$S_{CO} = \frac{F_{CO}}{F_{CO,out} + F_{CO2,out}} \times 100\% \quad (3)$$

$$S_{H2} = 0.5 \times \frac{F_{H2}}{F_{CO,out} + F_{CO2,out}} \times 100\% \quad (4)$$

3. Results and Discussion

3.1. XRD and TG-DTA Analysis. The chemical composition of the as-synthesized hydrotalcite samples is presented in Table 1. The compositions of these materials are similar to those obtained from analysis of the gel prior to calcination, suggesting the incorporation of cations within the HTLC structure. The nickel loading of all samples is slightly lower than the nominal values because of the loss of nickel during washing.

XRD studies show the structural evolution during thermal treatments as a function of calcination temperatures. Herein, we present data for NMA3-HT only as a typical example, as the phase evolution of hydrotalcites have been extensively studied previously.[10,33−35] The XRD data for NMA3-HT (Figure 1a) exhibits sharp and symmetrical Bragg reflections for the (0 0 3), (0 0 6), (1 1 0), and (1 1 3) planes and broad and asymmetric reflections for the (1 0 2), (1 0 5), and (1 0 8) planes, which is the characteristic of well-crystallized hydrotalcite with a rhombohedral structure (JSPDS:35-0965).[30] The absence of other phases suggests that both Ni^{2+} and Al^{3+} have isomorphically replaced Mg^{2+} cations in the brucite-like layers, which is

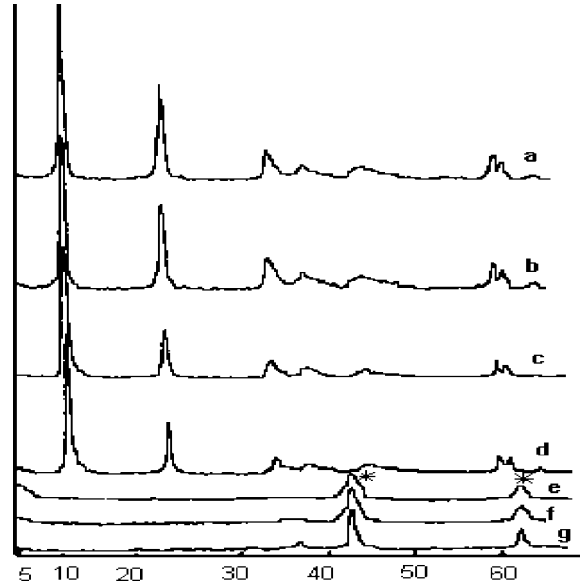

Figure 1. XRD data demonstrating the effects of thermal treatments on structure of hydrotalcite with Ni/Mg/Al = 1:11:2.4. Only Bragg peaks for hydrotalcites are apparent in data sets a−d, while data sets e−g show only MgO Periclase structure: (a) as-prepared; (b) 80 °C; (c) 150 °C; (d) 250 °C; (e) 350 °C; (f) 500 °C; (g) 800 °C.

(32) Song, C. *Catal. Today* **2006**, *115*, 2–32.

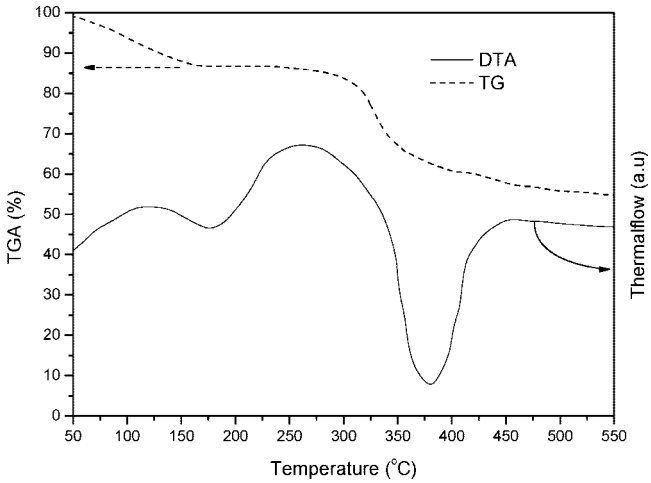

Figure 2. TG-DTA profiles of NMA3-HT hydrotalcite (heating rate 10 K/min, dashed line: thermogravimetric plot, solid line: differential scanning calorimetry curve).

reasonable given that the radius of Mg^{2+} and Ni^{2+} are very similar (0.65 and 0.72 Å, respectively). The layered structure of Ni−Mg/Al hydrotalcite is stable up to 250 °C as observed in Figure 1a−d, at which point the gradual decrease in intensity of the Bragg reflections suggests the gradual degradation of the lamellar hydrotalcite. XRD data for NMA3-HT calcined at 350 and 500 °C are illustrated in Figure 1, for example. It can be seen that the lamellar structure of hydrotalcite disappears after calcination above 350 °C, at which point it transforms to a poorly crystallized MgO periclase phase (JSPDS: 431022).[26] The crystallity of the periclase phase gradually increases with increasing calcination temperature, but at no point are (Ni)Mg/Al spinel or NiO observed. Indeed, the XRD data for a variety of transition metal substituted Mg/Al hydrotalcites only presented single phase periclase for samples, up to 800 °C.[26,36] In this case, the XRD data indicate that both nickel and aluminum oxides are incorporated into the MgO matrix with no significant segregation of other crystal species apparent. This high dispersion of Ni and Mg/Al is desirable for methane conversion to syngas.[24]

The TG-DTA profiles of NMA3-HT hydrotalcite are shown in Figure 2. Initial weight loss for the temperature range 50 °C up to 250 °C is assigned to the loss of physisorbed water and interlayer water molecules (DTA endotherm 185 °C). As confirmed by the XRD data shown in Figure 2c, the lamellar structure of NMA3-HT hydrotalcite is still maintained at 185 °C. The second thermal event takes place between 270 and 450 °C and is assigned to the removal of hydroxyl water together with the decomposition of intercalated nitrate anions.[3] In this stage, the layered structure is gradually collapsed during the heating process. The other Ni-based hydrotalcites show essentially similar TG-DTA profiles and are not reported here. Kloprogge and Frost[37] reported a similar change in the thermal transformation of Mg−Al HT using DT/TGA and infrared emission spectroscopy (IES). Their IES results show major changes in the temperature range of 350−450 °C, suggesting the end of the dehydroxylation. It has been reported[30] that the

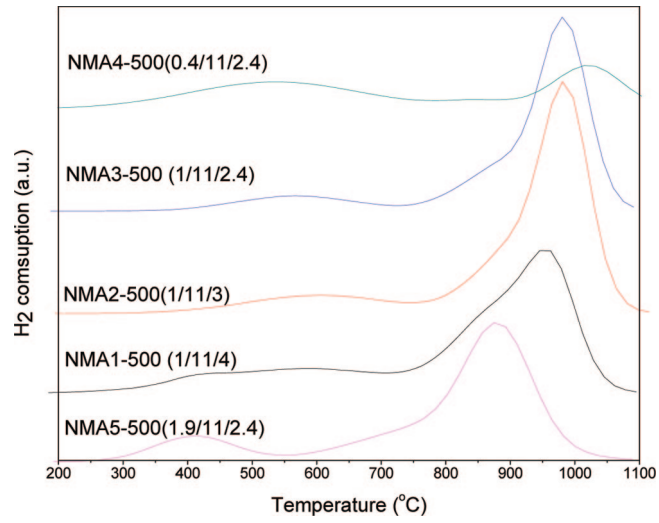

Figure 3. TPR profiles of Ni−Mg/Al(O) mixed oxides calcined at 500 °C. Figures in brackets represent the Ni/Mg/Al molar ratios obtained from ICP-AES.

Table 2. Composition, TPR, and TPD Results of Ni^0/ Mg Al(O)-500 Oxides[a]

sample	Ni wt %[a]	MgO wt %[a]	Al_2O_3 wt %[a]	H_2 uptake/Ni (molar ratio)	total CO_2 desorption (mmol/g)
NMA1-500	7.9	66.1	24.0	1.22	0.84
NMA2-500	8.2	70.5	19.3	1.13	0.72
NMA3-500	8.4	73.7	15.8	1.08	0.81
NMA4-500	3.6	78.0	17.4	0.40	0.88
NMA5-500	15.5	66.1	14.9	1.10	-

[a] Note: weight percentages are calculated according to the Ni^0/ MgO-Al_2O_3 ratio obtained from ICP-AES.

stability of higher molar fractions of Mg/Al in hydrotalcites is superior to the Ni−Mg/Al hydrotalcite with the same M^{2+}/M^{3+} molar ratio. Our results are consistent with these reports.

3.2. TPR of the Ni−Mg/Al(O) Mixed Oxides Derived from Ni-Based Hydrotalcites. Figure 3 presents the H_2-TPR profiles of the Ni−Mg/Al(O) catalysts derived from calcination of the corresponding Ni−Mg/Al ternary hydrotalcite at 500 °C. All of the catalysts exhibit a broad reduction peak from 700 to 1100 °C, which is assigned to the reduction of Ni^{2+} in the matrixes of mixed oxides.[38] The measured reduction temperature of pure NiO is around 340 °C. The reduction temperatures of Ni−Mg/Al(O) mixed oxides are higher than that for pure NiO because of the formation of MgO solid solution or spinel, which was a typical feature of catalysts derived from hydrotalcite-like compounds. The calculated H_2/Ni molar ratios are listed in Table 2 based on the H_2 uptake from integration of TPR profiles. The H_2/Ni molar ratios are well above stoichiometry for all samples except for NMA4-500. This is tentatively assigned to the presence of NiO_{1+x}, with a mixture of Ni^{2+} and Ni^{3+} cations, and coexistent impurities identified in previous research.[30]

For the NMA1-500, NMA2-500, and NMA3-500 samples, it can be seen (Figure 3) that the onset temperatures of reduction and the temperature of maximum reduction gradually shift to higher temperatures as Mg wt % increases. This implies that there is strong interaction among Ni/Mg/Al ions in the catalyst matrix, and this interaction increases as the Mg wt % increases, hindering the reduction of the NiO species in the catalysts. This difficulty of reduction Ni favors resistance to catalyst sintering and consequently helps to retain a high dispersion and finite

(33) Rivera, J. A.; Fetter, G.; Jiménez, Y.; Xochipa, M. M.; Bosch, P. *Appl. Catal., A* **2007**, *316*, 207–211.
(34) Perez-Lopez, O. W.; Senger, A.; Marcilio, N. R.; Lansarin, M. A. *Appl. Catal., A* **2006**, *303*, 234–244.
(35) Obalová, L.; Jirátová, K.; Kovanda, F.; Valášková, M.; Balabánová, J.; Pacultová, K. *J. Mol. Catal. A* **2006**, *248*, 210–219.
(36) Wang, Z.; Shangguan, W.; Su, J.; Jiang, Z. *Catal. Lett.* **2006**, *112*, 149–154.
(37) Theo Kloprogge, J.; Frost, R. L. *Appl. Catal., A* **1999**, *184*, 61–71.
(38) Djaidja, A.; Libs, S.; Kiennemann, A.; Barama, A. *Catal. Today* **2006**, *113*, 194–200.

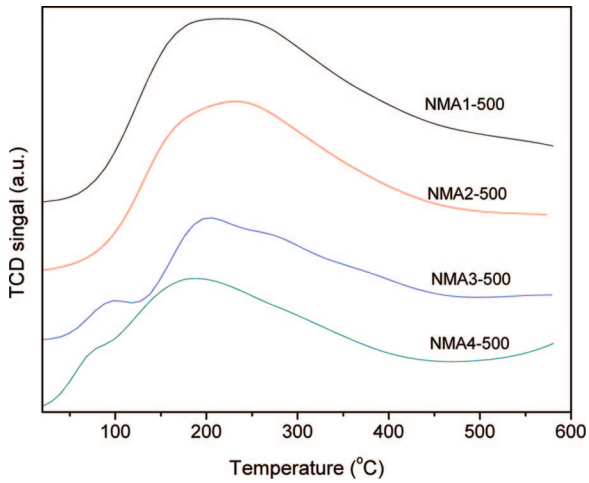

Figure 4. CO_2 TPD of Ni−Mg/Al(O) derived from NI−Mg/Al ternary hydrotalcites.

size of Ni^0. To investigate the effect of Ni loading on the redox property of the catalysts, we designed the catalysts with a fixed Mg/Al molar ratio of 11:2.4 and varied the molar ratios of Ni to be 0.4 (NMA4-500), 1.0 (NMA3-500), and 1.9 (NMA5-500). The reduction maximum of these samples steadily shifts to lower temperature when the Ni-loading increases. This suggests the increase of Ni loading leads to the dramatic decrease of Ni dispersion and thus to the decrease of the interactions among Ni and the Mg/Al in the catalyst matrix.

Besides the maximum reduction peak, a small reduction peak between 350 to 500 °C can be observed in Figure 3. This reduction temperature is nearly identical to that of pure NiO. Perez-Lopez and co-workers[34] observed a similar phenomenon for $Ni/MgAl_2O_4$ methane reforming catalysts and attributed it to the reduction of isolated NiO on Mg/Al mixed oxide supports. Our results suggest that isolated NiO is slightly influenced by the nature of the Mg/Al oxide support.

3.3. CO_2 TPD (Temperature-Programmed Desorption) of the Ni−Mg/Al(O) Mixed Oxides Derived from Ni-Based Hydrotalcites. CO_2-TPD measurements were conducted to test the surface basicity of the oxide catalysts. The obtained CO_2-TPD profiles of the calcined ternary hydrotalcite compounds are depicted in Figure 4. The amounts of CO_2 (Table 2) desorbing in the different temperature ranges (50−150 C, 150−450 °C, >450 °C) were calculated from the TPD curves in Figure 3. As the Al content increases (Ni/Mg/Al= 1/11/x, x = 2.4, 3, 4 for NMA3 to NMA1, respectively), the overall CO_2 desorption amounts decrease slightly, which is indicative of a decrease in surface basicity of the catalysts. The temperature of desorption maximum, corresponding to the presence of strong basic sites, is remarkably related to the composition of the samples, and here an increase of Mg wt % in the samples (increasing from NMA1 to NMA4) results in a shift of the CO_2 desorption peak to lower temperature. This suggests that Al cations in the materials contribute to strong basic sites as a consequence of a synergistic effect between Mg−Al.[39,40] Obalová et al. [35] proposed an exponential relationship between the surface basicity and reducibility for the NiMg(Mn)Al mixed oxide catalysts derived from ternary hydrotalcite with high Ni-contents. According to CO_2-TPD results and modified Sanderson

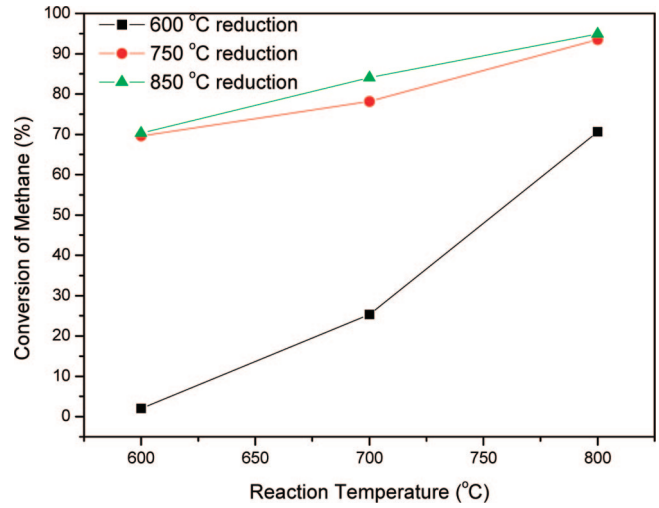

Figure 5. Plot of the influence of reduction temperature on the conversion of CH_4 over the NMA1-500 for three sample reduced at 600 °C (black line - square symbols), 750 °C (red line -circle symbols), and 850 °C (green line - triangle symbols).

Table 3. POM Reaction Results over the Ni-Based Catalysts

sample	T_{Red} (°C)	T_{React} (°C)	X_{CH4} (%)	X_{O2} (%)	Y_{CO2} (%)	Y_{CO} (%)	Y_{H2} (%)	S_{CO} (%)	S_{H2} (%)
NMA1-500	600	600	2.0	3.5	1.3	0.7	1.9	33.3	96.0
		700	25.3	75.5	12.4	12.9	6.2	51.0	24.8
		800	70.7	89.1	8.2	64.5	63.6	88.8	87.5
NMA1-500	750	600	69.6	99.5	11.8	57.8	60.6	83.0	87.0
		700	78.2	99.0	9.9	68.4	72.8	87.4	93.0
		800	93.5	98.6	4.0	89.6	93.0	95.8	99.4
NMA1-500	850	600	70.3	99.1	17.8	52.5	64.9	74.6	92.2
		700	84.1	98.7	10.9	73.2	87.3	87.0	103.1
		800	94.9	98.9	4.3	90.6	95.0	95.4	100.1

theoretical prediction, Rodrigues[41] classified the surface basicity of ternary oxides derived from hydrotalcites into four types depending on the coordination environment of surface oxygen and metal composition. For sample NMA1, 2, 3-500, the Ni wt % are very similar and relatively low in wt %, so that the difference of surface basicity can be attributed to the changes of Mg/Al ratio rather than to changes in Ni content. Moreover, the weak CO_2-TPD peaks in the 50−150 °C on the NMA3-500 and NMA4-500 samples can be associated with physisorption, suggesting that some weak basic sites exist on the surfaces of the materials.[41] This type of weak alkaline site has all but disappeared in the samples with higher Al loading. Moreover, CO_2-TPD at high temperature (450−600 °C) can be attributed to the thermal decomposition of carbonates formed during CO_2 adsorption.

3.4. Reactivity of Methane Partial Oxidation. *3.4.1. Influence of Reduction and Reaction Temperatures.* Because the metallic Ni is the active component for methane partial oxidation,[6] the reduction temperature of the oxides will play a key role for their POM performance. Taking NMA1-500 as an example, the influence of the reduction and reaction temperature on its methane conversion is illustrated in Figure 5. Here, the higher reduction temperatures (750 and 800 °C) favor methane conversion, the selectivity of CO and H_2, and also promote O_2 conversion (Table 3), as a result of the increase in concentration of Ni^0 active sites produced by the more vigorous reduction conditions at higher temperatures. Moreover, as the reaction temperature is increased, the reactivity of the sample reduced at 600 °C increases to a much greater degree than for those

(39) McKenzie, A. L.; Fishel, C. T.; Davis, R. J. *J. Catal.* **1992**, *138*, 547–561.
(40) Jiang, D.-e.; Zhao, B.; Xie, Y.; Pan, G.; Ran, G.; Min, E. *Appl. Catal., A* **2001**, *219*, 69–78.
(41) Rodrigues, A. *J. Math. Chem.* **2006**, *39*, 541–549.

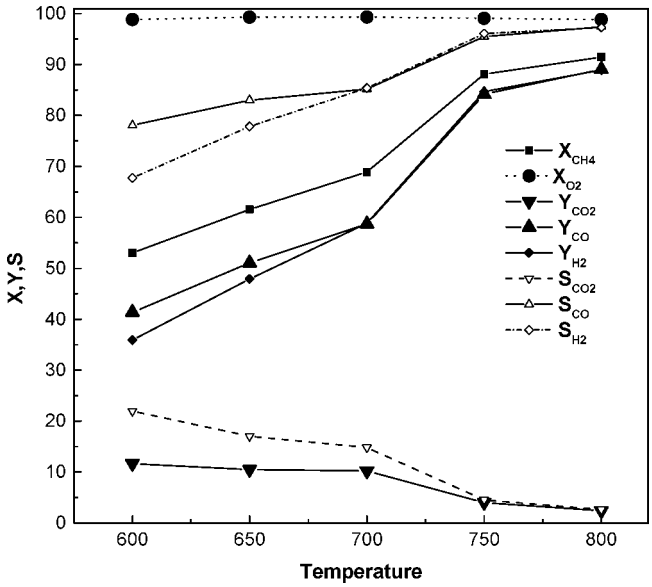

Figure 6. Effect of reaction temperature on POM of the NMA3-500 catalyst (X: conversion, S: selectivity, Y: yields).

samples reduced at 750 and 800 °C. In addition to the thermodynamic factors, this phenomenon can be partially attributed to in situ reduction of the sample (reduced at 600 °C) in the reaction process since the products are mainly reductive H_2 and CO gases. The in situ reduction of NiO species supported on Al_2O_3 has previously reported by Zhang and co-workers in a fluidized-bed methane-CO_2 reforming reaction.[42] This in situ reduction phenomenon suggests partial reduction of Ni-based catalysts is acceptable for a high temperature POM reaction catalyst, and hence, reduction at 750 °C is identified as the optimum reduction conditions for our materials.

Figure 6 depicts the effect of reaction temperature on the POM performance taking the NMA3-500 sample reduced at 750.°C as a example. It can be seen that the conversion of reactants (CH_4 and O_2) and the yields of the products (CO and H_2) increase with increasing reaction temperature. However, the yield and selectivity of CO_2 in the resultant gases decrease as the reaction temperature increase. The result implies the partial oxidation of methane, probably via a 2-step reaction mechanism. Methane is first combusted in the oxygen to produce CO_2 and H_2O and release heat, and then the residential methane reforms the CO_2 and H_2O to give syngas.

3.4.2. Effects of Catalyst Composition. Table 4.shows the POM performance at 750 °C over the various catalysts reduced at 750 °C. All the catalysts show excellent reactivity for POM reaction except for NMA4-500 sample with 3.6 wt % Ni loading. The poor activity of NMA4-500 arises as a consequence of its low concentration of active sites (low Ni wt %) as discussed above (see Section 3.4.1). The reactivity and selectivity are nearly identical for the catalysts with Ni loading from 7.9 wt % to 15.5 wt %. These results suggest that 8 wt % Ni is the optimal Ni concentration for POM reactions using Ni/Mg−Al(O) catalysts, with the highest selectivity and conversion rates obtained for NMA3-500 (8.4 wt % Ni).

(42) Chen, X.; Honda, K.; Zhang, Z.-G. *Appl. Catal., A* **2005**, *279*, 263–271.

Table 4. Methane Partial Oxidation over Ni/Mg−Al(O) Catalysts Reduced and Reacted Both at 750 °C

sample	X_{CH4} (%)	X_{O2} (%)	Y_{CO} (%)	Y_{H2} (%)	S_{CO} (%)	S_{H2} (%)
NMA1-500	87.2	98.9	80.3	84.8	92.1	97.3
NMA2-500	87.5	98.9	81.8	84.7	93.4	96.8
NMA3-500	88.1	99.1	84.1	84.7	95.5	96.1
NMA4-500	12.3	33.3	6.9	4.4	56.4	35.9
NMA5-500	88.4	98.6	82.6	86.2	93.4	97.5

4. Conclusion

A simple co-precipitation method has been adopted to prepare Ni−Mg/Al ternary hydrotalcites with adjusted Ni/Mg/Al molar ratios (Ni/Mg/Al molar ratios are 1:11:4, 1:11:3, 1:11:2.4, 0.4:11:2.4, 1.9:11:2.4, respectively). The ternary hydrotalcites were used as precursors to prepare low Ni-loading catalysts for POM to syngas. The reducibility, surface basicity, and effects of catalyst reduction on POM reactivity for these catalysts have been explored in detail by XRD, TGA-DTA, and temperature-programmed catalytic activity experiments (TPR and CO_2-TPD). We have observed the following:

(1) The Mg/Al molar ratio significantly affects the reducibility of the catalysts.

(2) The Mg/Al molar ratio has little effect on the surface basicity with low Ni-loading, but a high Al content favors the strong basic sites of the catalysts because of the synergistic effects among the components.

(3) The Ni-loading concentration greatly affects the reducibility of the catalysts and slightly affects on the surface basicity, mainly on the weakly alkaline sites.

(4) The reduction temperature significantly affects the reactivity of the catalysts but in situ reduction of the catalyst has been observed during POM reaction at high temperature. The optimum reduction conditions have been established based on the compromise between catalyst reactivity and energy penalty.

(5) Under the optimized reaction conditions, the catalysts with Ni wt % in 8% to 15.5% show similar reactivity in POM reaction but a much higher one than for catalyst with lower Ni-loading (4 wt %). These results reveal that the Ni/Mg/Al ternary hydrotalcites are excellent precursor for effective Ni-based catalysts with low Ni-loading.

Acknowledgment. The authors thank Professor Can Li from Dalian Institute of Chemical Physics, CAS, for discussion during the preparation of this manuscript. We are grateful for his constructive suggestion to mimic the flue gas reforming process. Dr. Su and Jiang acknowledge the financial support of the Shandong Youth Scientist's Research Fund (2004BS08010).

EF800933J